

The Ureide-Degrading Reactions of Purine Ring Catabolism Employ Three Amidohydrolases and One Aminohydrolase in Arabidopsis, Soybean, and Rice^{1[W]}

Andrea K. Werner², Nieves Medina-Escobar², Monika Zulawski, Imogen A. Sparkes³, Feng-Qiu Cao, and Claus-Peter Witte*

Freie Universität Berlin, Dahlem Centre of Plant Sciences, Department of Plant Biochemistry, 14195 Berlin, Germany (A.K.W., N.M.-E., M.Z., F.-Q.C., C.-P.W.); and Oxford Brookes University, School of Life Sciences, Oxford OX3 0BP, United Kingdom (I.A.S.)

ORCID ID: 0000-0002-3617-7807 (C.-P.W.).

Several ureides are intermediates of purine base catabolism, releasing nitrogen from the purine nucleotides for reassimilation into amino acids. In some legumes like soybean (*Glycine max*), ureides are used for nodule-to-shoot translocation of fixed nitrogen. Four enzymes of Arabidopsis (*Arabidopsis thaliana*), (1) allantoinase, (2) allantoate amidohydrolase (AAH), (3) ureidoglycine aminohydrolase, and (4) ureidoglycolate amidohydrolase (UAH), catalyze the complete hydrolysis of the ureide allantoin in vitro. However, the metabolic route in vivo remains controversial. Here, in growth and metabolite analyses of Arabidopsis mutants, we demonstrate that these enzymes are required for allantoin degradation in vivo. Orthologous enzymes are present in soybean, encoded by one to four gene copies. All isoenzymes are active in vitro, while some may be inefficiently translated in vivo. Surprisingly, transcript and protein amounts are not significantly regulated by nitrogen fixation or leaf ureide content. A requirement for soybean AAH and UAH for ureide catabolism in leaves has been demonstrated by the use of virus-induced gene silencing. Functional AAH, ureidoglycine aminohydrolase, and UAH are also present in rice (*Oryza sativa*), and orthologous genes occur in all other plant genomes sequenced to date, indicating that the amidohydrolase route of ureide degradation is universal in plants, including mosses (e.g. *Physcomitrella patens*) and algae (e.g. *Chlamydomonas reinhardtii*).

Plants are often growing under nitrogen-limiting conditions and possess means to optimize the use of available nitrogen by redistributing it from source to sink tissues (Masclaux-Daubresse et al., 2010). Most nitrogen is stored in proteins, but also the nucleobases are rich in nitrogen. Both nitrogen stores are subject to redistribution, indicated by the progressive decrease of protein as well as RNA content of leaves from full expansion to senescence (Masclaux et al., 2000). Plants possess enzymes that can convert nucleobase nitrogen into amino acid nitrogen, which is usually used for long-distance nitrogen transport. For this conversion, the pyrimidine bases, uracil and thymine, are catabolized in

three enzymatic steps, which are followed by ammonia reassimilation as well as transamination reactions to incorporate the nitrogen into amino acids in Arabidopsis (*Arabidopsis thaliana*; Zrenner et al., 2009). The catabolism of the purine ring from the nucleotides AMP and GMP converges on xanthine, for which a degradation pathway involving eight enzymatic reactions has been suggested in Arabidopsis (for review, see Werner and Witte, 2011). In the cytosol, xanthine is converted to uric acid by xanthine dehydrogenase (Hesberg et al., 2004). After import into the peroxisome, uric acid is oxidized by urate oxidase to 5-hydroxyisourate, which is converted in a two-step reaction to the ureide S-allantoin by the peroxisomal allantoin synthase (Lamberto et al., 2010). The next enzyme, allantoinase (ALN), resides in the endoplasmic reticulum (ER; Werner et al., 2008), hydrolyzing S-allantoin to allantoate (Fig. 1A; Supplemental Fig. S1). A corresponding transfer DNA (T-DNA) insertion mutant of Arabidopsis does not grow on allantoin as sole nitrogen source (Yang and Han, 2004) and accumulates allantoin in vivo (Todd and Polacco, 2006; Werner et al., 2008).

Three additional enzymes have been described that are capable of catabolizing allantoate in vitro to glyoxylate, two molecules of carbon dioxide, and four molecules of ammonia (Werner et al., 2010; Fig. 1A; Supplemental Fig. S1). (1) Allantoate amidohydrolase (AAH) hydrolyzes allantoate to S-ureidoglycine. The enzymes of Arabidopsis and soybean (*Glycine max*) reside in the ER (Werner et al., 2008). The corresponding

¹ This work was supported by the Deutsche Forschungsgemeinschaft (grant no. DFG WI3411/1-2) and the German Academic Exchange Service from funds of the German Federal Ministry for Education and Research, German-Chinese Research Groups program, and by the Scholarship Program of the Chinese Scholarship Council (grant no. [2007]3020) and the Centre for International Collaboration of the Freie Universität Berlin (to F.-Q.C.).

² These authors contributed equally to the article.

³ Present address: University of Exeter, College of Life and Environmental Sciences, Stocker Road, Exeter EX4 4QD, UK.

* Address correspondence to cpwitte@zedat.fu-berlin.de.

The author responsible for distribution of materials integral to the findings presented in this article in accordance with the policy described in the Instructions for Authors (www.plantphysiol.org) is: Claus-Peter Witte (cpwitte@zedat.fu-berlin.de).

^[W] The online version of this article contains Web-only data.

www.plantphysiol.org/cgi/doi/10.1104/pp.113.224261

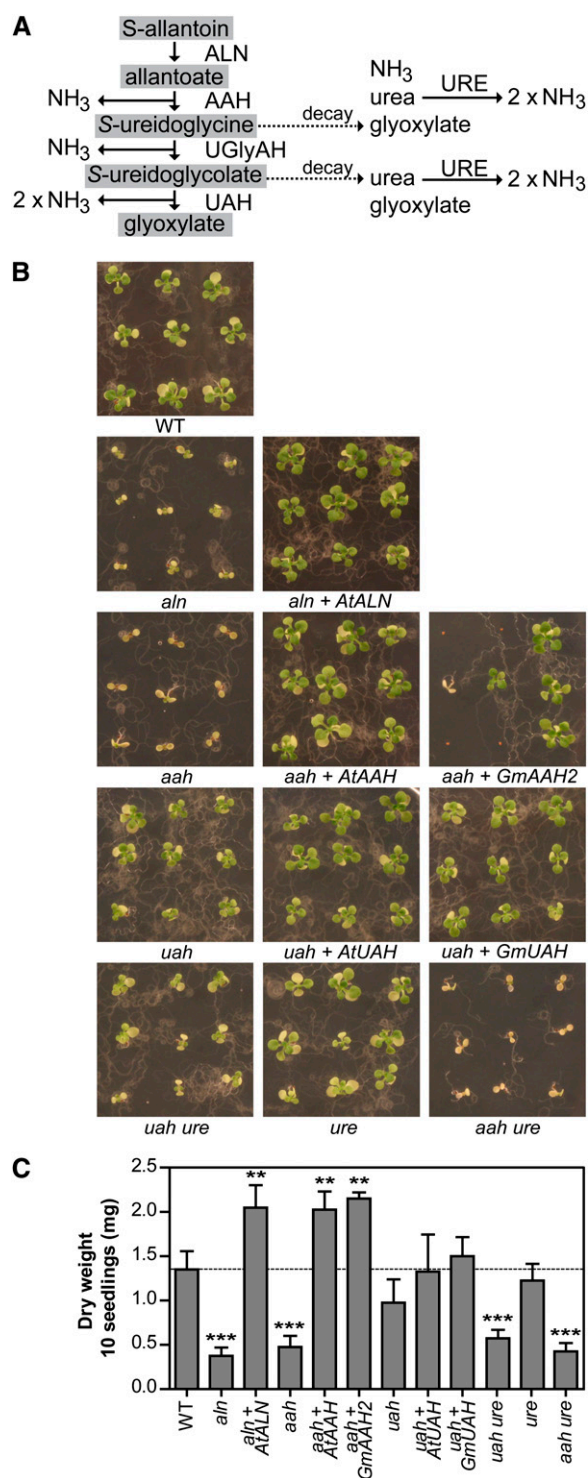


Figure 1. Schematic model of ureide catabolism, and growth analysis of mutants with allantoin as nitrogen source. A, Schematic model of S-allantoin degradation in plants by enzymatic and nonenzymatic pathways focused on ammonia release. B, Arabidopsis wild type (WT), mutants, and complementation (overexpression) lines grown for 6 weeks on agar medium with 10 mM allantoin as sole nitrogen source. C, Dry weight of plants shown in B; error bars are sd of four biological replicates. Statistical evaluation used ANOVA coupled with a Dunnett posttest comparing with the wild type (* $P < 0.05$, ** $P < 0.01$, and *** $P < 0.001$).

mutants of *Arabidopsis* accumulate allantoate while showing a growth defect when allantoin is used as sole nitrogen source, demonstrating that AAH is essential for allantoate catabolism in this plant (Todd and Polacco, 2006; Werner et al., 2008). (2) Ureidoglycine aminohydrolase (UGlyAH), located in the ER, cleaves S-ureidoglycine hydrolytically to S-ureidoglycolate and ammonia in vitro (Serventi et al., 2010; Werner et al., 2010). Ureidoglycine is unstable and decays in the absence of an enzyme with a half-life of a few minutes to glyoxylate, ammonia, and urea (Fig. 1A). (3) The last enzyme, ureidoglycolate amidohydrolase (UAH), was shown to hydrolyze S-ureidoglycolate in vitro, giving rise to glyoxylate, carbon dioxide, and two molecules of ammonia (Werner et al., 2010). This reaction proceeds presumably via an S-hydroxyglycine intermediate that decomposes nonenzymatically to glyoxylate and ammonia (Werner and Witte, 2011). In the absence of an enzyme, ureidoglycolate decays with a half-life of a few hours to glyoxylate and urea (Gravenmade et al., 1970; Fig. 1A). So far, it has not been demonstrated that UGlyAH and UAH are involved in ureide catabolism in vivo. Especially controversial is the nature of the ureidoglycolate-degrading reaction. From chickpea (*Cicer arietinum*) and common bean (*Phaseolus vulgaris*), enzymes were purified that, in contrast to UAH, cleave ureidoglycolate to glyoxylate and urea (Muñoz et al., 2001, 2006). Consistently, it was reported that in soybean, half of the nitrogen from allantoate was released as urea, presumably during ureidoglycolate degradation (Todd and Polacco, 2004). However, earlier studies could not find any evidence for a urea intermediate in the course of ureide catabolism in soybean (Winkler et al., 1985, 1987; Stebbins and Polacco, 1995).

Soybean belongs to a certain class of legumes (including species from *Glycine*, *Vigna*, and *Phaseolus*) known as ureide exporters in which ureide catabolism plays a special role (Schubert, 1986). Symbiotically fixed nitrogen is incorporated mainly into purine nucleotides, which are catabolized to ureides (allantoin and allantoate) in the nodules. The ureides are exported from the nodules via the xylem (Collier and Tegeder, 2012) to feed the shoot with nitrogen (Schubert, 1981). To access the nitrogen, the ureides must be hydrolyzed, generating ammonia for reassimilation into amino acids. Because of this special role of ureide catabolism in some legumes, it is conceivable that these plants may employ an enzymatic pathway for this metabolic task that differs from that found in other plants.

RESULTS

Analysis of Arabidopsis Mutants

Arabidopsis grows on allantoin as sole nitrogen source (Desimone et al., 2002; Fig. 1B). T-DNA insertions in the ureide catabolic genes *ALN* and *AAH* abolish growth beyond germination, because ammonia cannot

be generated from allantoin in these mutants. This phenotype is complemented by the introduction of the respective complementary DNAs under the transcriptional control of the 35S promoter into the corresponding mutant backgrounds (Fig. 1, B and C; Todd and Polacco, 2006; Werner et al., 2008). In contrast, the growth of the *uah* mutant, which lacks *UAH* mRNA (Supplemental Fig. S2), appears only slightly reduced (Fig. 1B). A statistically significant reduction in seedling dry weight was not observed (Fig. 1C), although the *UAH* reaction is required to obtain half of the ammonia from allantoin according to our model (Fig. 1A). This observation can be explained if one considers that the substrate of *UAH*, *S*-ureidoglycolate, is an unstable compound that decomposes to glyoxylate and urea with a half-life of only a few hours (Gravenmade et al., 1970). It is possible that the *UAH* reaction is bypassed if the ER-born urea from nonenzymatic ureidoglycolate decay can reach the cytosol, where it is hydrolyzed by urease (*URE*) to carbon dioxide and ammonia (Fig. 1A). A *uah ure* double mutant was generated to test this hypothesis, and indeed, this mutant displayed a significant growth reduction while both respective single mutants did not (Fig. 1, B and C).

A metabolite analysis of wild-type and mutant plants grown on soil with nitrate as nitrogen source was performed. The *aln* mutant had an elevated allantoin content, as observed previously (Todd and Polacco, 2006). It accumulated $0.52 \pm 0.04 \mu\text{mol}$ allantoin g^{-1} fresh weight (about 10-fold more than the wild type). In contrast, the downstream metabolites allantoin and ureidoglycolate were nearly absent (Fig. 2, A and B), while the concentrations of these metabolites in the corresponding complementation line (*aln + AtALN*) were similar to the concentration in the wild type. In the *aah* mutant, the substrate allantoin accumulated to about 5-fold the amount found in the wild type (Fig. 2A; Todd and Polacco, 2006; Werner et al., 2008), while the downstream metabolite ureidoglycolate was depleted. The complementation lines (*AtAAH* and *GmAAH2* in the *aah* background) had a reduced allantoin content compared with the wild type (Werner et al., 2008), but the ureidoglycolate concentrations were not altered (Fig. 2, A and B). Most significantly, the ureidoglycolate content was increased approximately 2-fold in the *uah* mutant, while it was strongly reduced in the respective complementation lines (*AtUAH* and *GmUAH* in the *uah* background; Fig. 2B). The postulated bypass of the *UAH* reaction via *URE* was confirmed by the significantly increased urea content in the *uah ure* double mutant, not observed in the *uah* mutant and less prominent in the *ure* single mutant and in the *aah ure* double mutant (Fig. 2C). The latter line served as a control to ensure that the disruption of ureide catabolism in the *URE* negative background in general (at a different point than at *UAH*) is not sufficient to increase urea concentrations beyond the level observed in the *ure* single mutant.

In summary, this growth and metabolite analysis demonstrates that *UAH* of *Arabidopsis* acts downstream

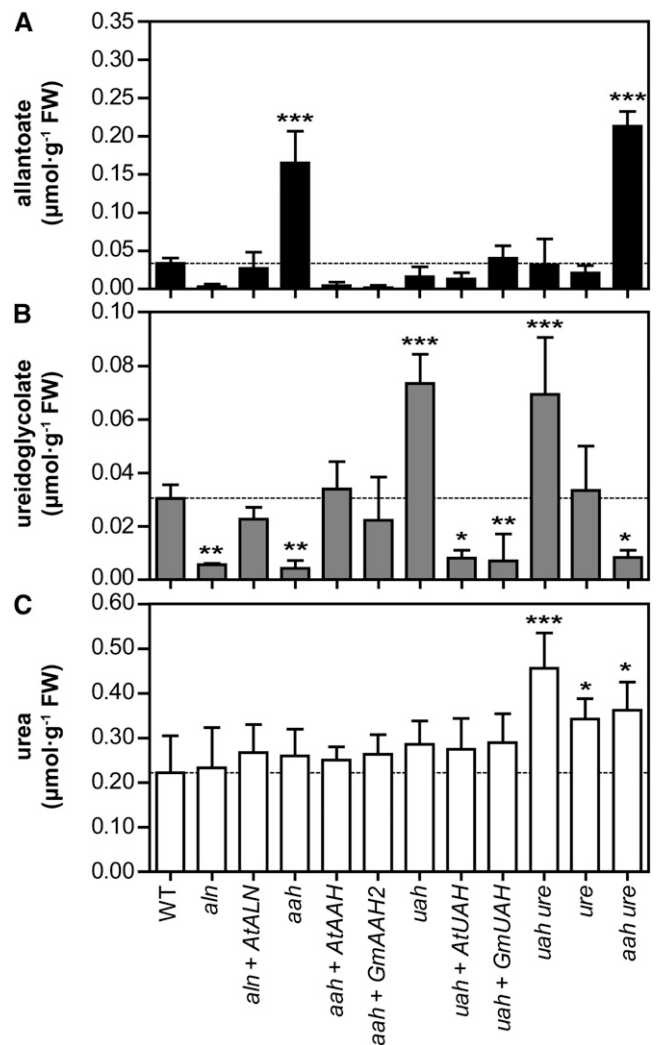


Figure 2. Metabolite analysis of ureide catabolic mutants and complementation (overexpression) lines supplied with nitrate as nitrogen source. Allantoin (A), ureidoglycolate (B), and urea (C) concentrations in the rosette are shown with reference to fresh weight (FW). Error bars are SD of three biological replicates. Statistical evaluation is as in Figure 1. WT, Wild type.

of *ALN* and *AAH* in the catabolism of allantoin *in vivo*. This finding implies that *UGlyAH* must be involved *in vivo* as well, because it has been shown that *AAH* will generate *S*-ureidoglycolate, the substrate of *UAH*, only in concert with *UGlyAH* (Serventi et al., 2010; Werner et al., 2010).

Functional Assessment of the Ureide Catabolic Enzymes of Soybean and Rice

Using the amino acid sequences of the ureide catabolic enzymes from *Arabidopsis* as query, four putative orthologs for *ALN*, two for *AAH*, two for *UGlyAH*, and two for *UAH* can be found in the soybean proteome deduced from the genomic sequence. Putative orthologous genes for these enzymes are present in all sequenced

plant genomes, mostly in single copy, and occur as well in mosses such as *Physcomitrella patens* and algae such as *Chlamydomonas reinhardtii* (Supplemental Figs. S3–S6).

Coding sequences of the soybean genes for AAH2, UGlyAH1, and UAH were cloned, and the corresponding proteins were transiently expressed in *Nicotiana benthamiana* as C-terminally StrepII-tagged variants for affinity purification (Supplemental Fig. S7). Together, the three purified enzymes released 4 mol of ammonia from allantoate in vitro (Fig. 3, mix A), whereas AAH alone or in concert with UAH (mixes B and C) only led to the release of 2 mol ammonia, one from the AAH reaction and one from the rapid nonenzymatic decay of *S*-ureidoglycine to ammonia, urea, and glyoxylate (Fig. 1A). In the presence of UGlyAH, *S*-ureidoglycine did not decay but was enzymatically converted to ammonia and *S*-ureidoglycolate, the substrate of UAH (mix D). Without AAH, neither UGlyAH nor UAH was able to release ammonia from allantoate (Fig. 3, mix E). Identical enzymatic conversions of allantoate were observed with the orthologous enzymes from Arabidopsis (Werner et al., 2010). Candidate enzymes of AAH, UGlyAH, and UAH from rice (*Oryza sativa*) were cloned, expressed, and purified in the same manner, and their corresponding activities were confirmed (Supplemental Fig. S8; Table I). Taken together, these data demonstrate that the enzymes of ureide catabolism are functional in soybean and rice and that genes coding for orthologous enzymes are universally present in plants.

Are there several copies of these genes in soybean because this plant has an additional special requirement for ureide catabolism during nitrogen fixation? By sequence analysis, this possibility can be excluded for UAH because the second copy of the gene (*UAH2*) contains a nonsense codon in the reading frame (Supplemental Fig. S6), leaving only *UAH1* as a functional copy (and therefore called simply UAH). The

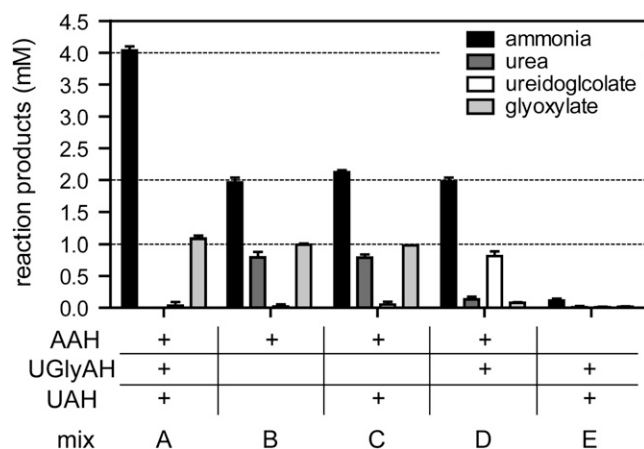


Figure 3. Complete conversion of allantoate into the respective end products in the presence of different combinations of ureide-degrading enzymes from soybean. Allantoate (1 mM) was incubated with the respective enzymes for 80 min. Error bars are SD of three independent measurements.

Table 1. Kinetic constants

Protein	K_m	Specific Activity	k_{cat}	Catalytic Efficiency
	μM	units mg^{-1}	s^{-1}	$\text{s}^{-1} \text{M}^{-1}$
AtALN	5,472	973	879	1.61×10^5
GmALN1	11,758	1,596	1,484	1.26×10^5
GmALN2	15,251	3,678	3,423	2.24×10^5
GmALN3	13,118	82	76	5.81×10^3
GmALN4	17,089	761	701	4.11×10^4
GmAAH1	72	43	37	0.52×10^6
GmAAH2	102	39	34	0.33×10^6
OsAAH	83	91	78	0.94×10^6
GmUAH	40	20	17	4.30×10^5
OsUAH	188	64	55	2.95×10^5

catalytic efficiency of UAH from soybean (Table I) is similar to that of the corresponding enzyme from Arabidopsis ($2.0 \times 10^5 \text{ s}^{-1} \text{ M}^{-1}$; Werner et al., 2010). The two *AAH* copies and the two *UGlyAH* copies appear to code for functional proteins based on sequence analysis in silico (Supplemental Figs. S4 and S5). Functional testing of the two *AAH* enzymes affinity purified from *N. benthamiana* after transient expression showed that both are active and have similar catalytic efficiencies (Table I) comparable to the catalytic efficiency of the Arabidopsis enzyme ($0.9 \times 10^6 \text{ s}^{-1} \text{ M}^{-1}$; Werner et al., 2008). Both *UGlyAH* variants were active as well, leading to accelerated enzymatic ammonia release from ureidoglycine generated by *AAH* in a coupled reaction (Supplemental Fig. S9). Enzymatic constants for *UGlyAH* were not determined because its substrate, *S*-ureidoglycine, is unstable and commercially not available. Next, the four *ALN*s were investigated. The *ALN* genes were numbered according to Duran and Todd (2012). All four corresponding proteins, affinity purified after transient expression, displayed *ALN* activity, but *ALN1* and *ALN2* possessed a severalfold higher catalytic efficiency (similar to that of *ALN* from Arabidopsis) than *ALN3* and *ALN4* (Table I). In summary, these data show that the soybean genome codes for at least two equally functional copies of each of the ureide-degrading enzymes (with the exception of UAH). This finding is consistent with the possibility that certain isoenzymes are required especially for the degradation of ureides from nitrogen fixation.

Transcript and Protein Analysis

The transcripts for ureide-degrading enzymes were analyzed to further elucidate a potential role of certain isoenzymes in particular tissues or during nitrogen fixation. *ALN1* and *ALN2* are ubiquitously expressed, whereas *ALN3* and *ALN4* transcripts are most abundant in nodules and hardly present in other tissues (Fig. 4). This was observed as well by Duran and Todd (2012), who speculated that *ALN3* and *ALN4* might have a particular role in allantoin degradation in the nodule. 5'-RNA ligase-mediated-RACE experiments performed by us with leaf and nodule RNA revealed that the 5' leader sequences of *ALN3* and *ALN4* mRNAs

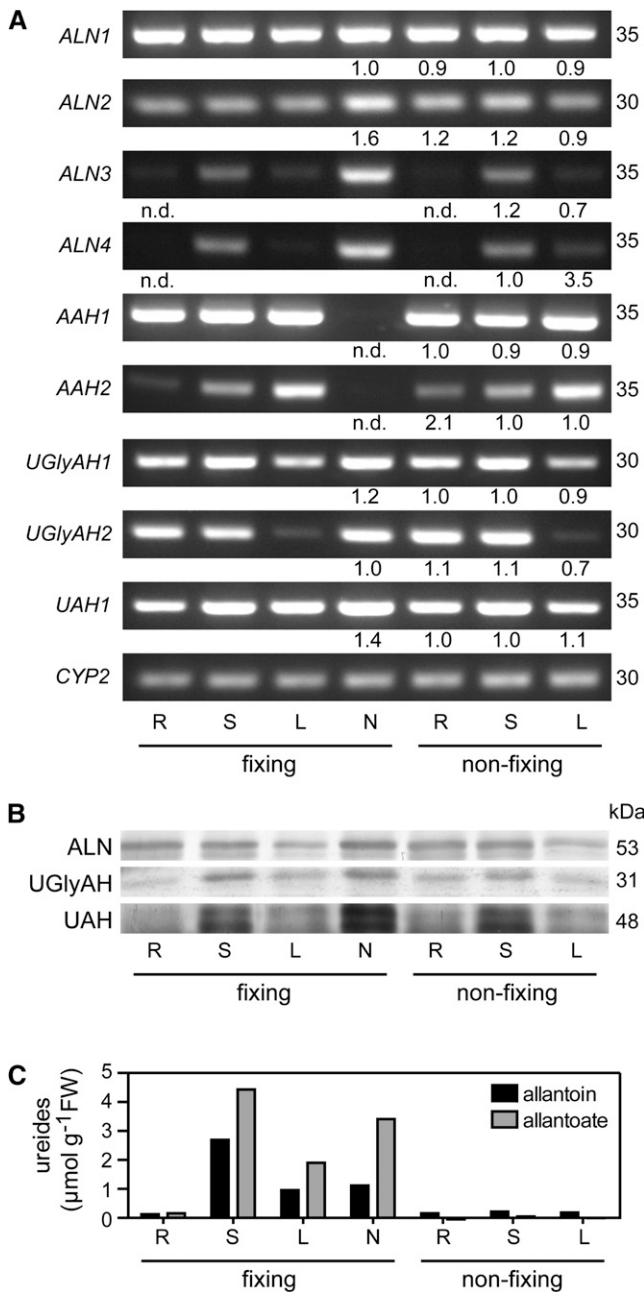


Figure 4. Expression analysis of ureide catabolic genes/proteins in different tissues of soybean plants under nitrogen fixing versus non-fixing conditions. A, Reverse transcription-PCR using different tissues of 5-week-old plants in the V2 to V3 stage growing either under fixing or nonfixing conditions. R, Root; S, stem; L, pool of all leaves; N, nodule. The transcript from the *CYP2* housekeeping gene (*Glyma12g02790*) served as a control. PCR cycle numbers are indicated at each panel. The factorial change of intensities from signals of the same tissue in fixing versus nonfixing conditions is given below each panel (quantified with ImageJ). The values for nodules were obtained by referring to root tissue under fixing conditions. n.d., Not detected. B, Western blot with ALN-, UGlyAH-, and UAH-specific antibodies. C, Ureide measurement to confirm the status of nitrogen fixation. FW, Fresh weight.

have a length of only 10 bp. The start codon of mRNAs with such short leader sequences is inefficiently recognized, leading to the preferential utilization of the next downstream AUG for the initiation of translation (Kozak, 1991; Hinnebusch, 2011). In *ALN3* and *ALN4* mRNA, however, the next downstream AUG codon is not in the reading frame of the allantoin coding sequence. The comparatively low catalytic efficiency (Table I), the generally low expression, and the short 5' leader sequence of the corresponding mRNAs together indicate that *ALN3* and *ALN4* are not contributing significantly to ALN activity in vivo, probably not even in the nodule where the transcripts for these isoforms are most abundant.

Both *AAH* genes are not transcribed in nodules, while the expression of *AAH2* is low in roots (Fig. 4). The former finding is consistent with a block of purine base catabolism at the stage of allantoate to facilitate the export of this ureide from the nodules. *UGlyAH1* is ubiquitously expressed while the expression of *UGlyAH2* is weak in leaves, indicating that *UGlyAH1* is the main enzyme for processing ureidoglycine in the leaf. *UAH* is well expressed in all investigated tissues. Publicly available RNAseq data for soybean are in agreement with the expression data presented here (Supplemental Fig. S10; Severin et al., 2010).

Surprisingly, the abundance of the transcripts for ureide-degrading enzymes was not markedly different in plants growing with or without nitrogen fixation (Fig. 4A). Similarly, the protein abundance of the ALNs, UGlyAHs, and UAH was not grossly altered depending on the source of nitrogen (Fig. 4B). Unfortunately, the abundance of the AAH protein was always too low for detection. The status of nitrogen fixation was confirmed by the high abundance of ureides in shoot, leaves, and nodules of plants, depending on nitrogen fixation and the absence of these compounds in plants growing without nitrogen fixation (Fig. 4C). Potential alterations in transcript abundance and protein amounts were investigated additionally in an experiment comparing transcripts and proteins from second and still expanding third trifoliate leaves of plants that were either growing with nitrogen fixation or without (Supplemental Fig. S11). This is particularly indicative, because the younger third leaves of plants relying on nitrogen fixation contained high amounts of ureides (and therefore potentially required particularly active ureide degradation), while the older second leaf did not contain elevated ureide amounts anymore, as also observed by Matsumoto et al. (1977b). As before, there were no gross differences in transcript amounts irrespective of leaf or status of nitrogen fixation. The protein quantities of ALN, UGlyAH, and UAH were generally higher in the younger leaf irrespective of whether the plant was relying on nitrogen fixation or not.

In summary, there does not seem to be a marked regulation of transcript or protein level of the ureide-degrading enzymes depending on the source of nitrogen or the abundance of ureides. A special role of particular isoenzymes for processing ureides generated during

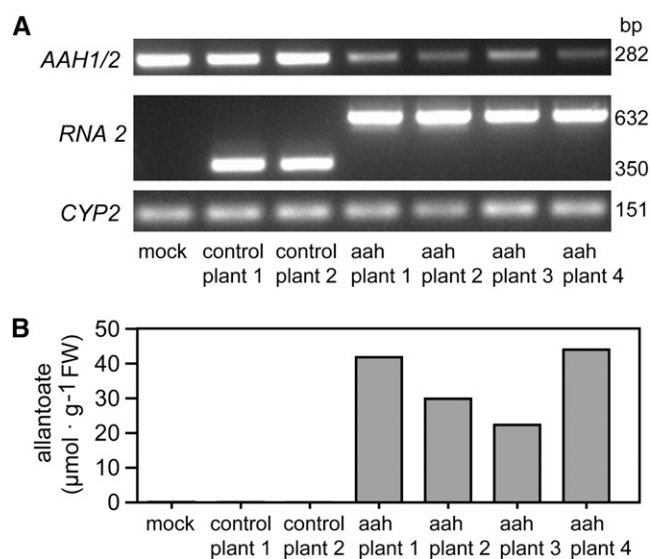


Figure 5. *AAH* silencing in soybean leaves and consequences on allantoate content. A, Reverse transcription-PCR using soybean RNA extracted from leaves of independent plants that were either mock inoculated (mock) or inoculated with DNA coding for wild-type *Bean pod mottle virus* (BPMV; control) or with DNA coding for BPMV-aah. B, Allantoate content of the leaves investigated in A. Values of individual leaves are shown. The allantoate content is significantly (Student's *t* test; $P = 0.0023$) different between controls and AAH-silenced leaves. FW, Fresh weight.

nitrogen fixation cannot be confirmed, at least for leaf tissue.

Ureide Degradation by AAH and UAH of Soybean in Vivo

Given the lack of clear regulation on the transcript and protein levels, it may be questioned whether the ureide-catabolizing enzymes presented here are involved in ureide degradation in soybean leaves in vivo. *GmAAH2* as well as *GmUAH* transgenes complement the corresponding mutants of *Arabidopsis* (Figs. 1 and 2), indicating that the respective enzymes are competent to function in ureide catabolism in vivo. Using bean pod mottle virus constructs (Zhang et al., 2010), *AAH1/AAH2* and *UAH* were silenced by virus-induced gene silencing (VIGS) in soybean plants. First, experiments were performed with nitrogen-fixing plants to investigate whether ureide catabolism is altered under these conditions. Unfortunately, VIGS failed to establish in young expanding leaves, which are the major sinks for the ureides produced in the nodules, likely because the migration of the virus and the silencing trigger were lagging behind leaf development (Juvale et al., 2012). However, it was possible to establish VIGS in middle-aged leaves, but these did not contain high ureide levels anymore (Matsumoto et al., 1977b). When *AAH* was silenced, allantoate accumulated in such leaves (Fig. 5), demonstrating that *AAH* carries out allantoate degradation in vivo. However, when

UAH was silenced, an accumulation of ureidoglycolate was not observed. Because VIGS generally results only in a partial knockdown of transcript, we speculated that residual *UAH* may suppress ureidoglycolate accumulation. Even in the *UAH*-null background of *Arabidopsis*, ureidoglycolate accumulation is comparatively weak because it decays nonenzymatically in vivo, as shown above (Fig. 2). To increase the flux through the ureide catabolic pathway, *UAH*-silenced leaves were fed racemic allantoate (10 mM solution) through the petiole. In leaves from plants infected with three distinct viral *UAH*-silencing constructs (spaced evenly along the *UAH* complementary DNA), ureidoglycolate accumulated under these conditions but not in the controls (Fig. 6), demonstrating that soybean *UAH* is indeed required for ureidoglycolate degradation in vivo.

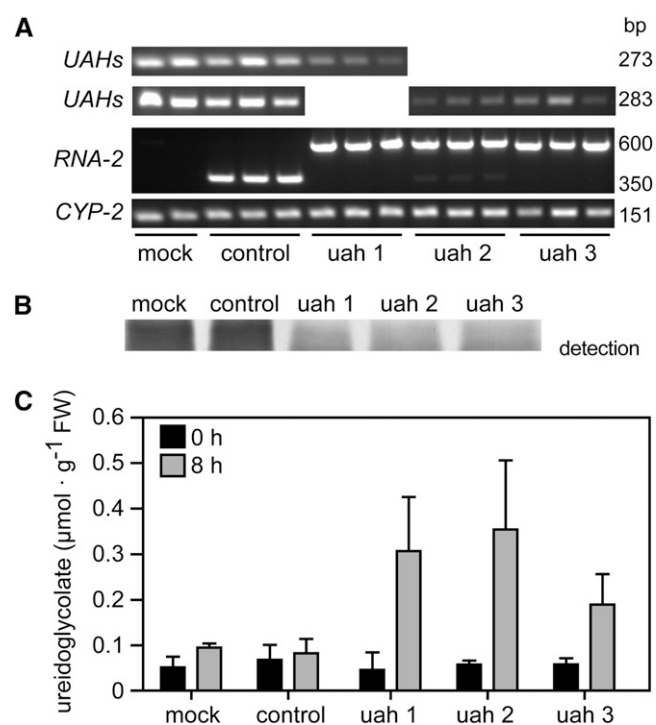


Figure 6. *UAH* silencing in soybean leaves and consequences for *UAH* protein concentration and for ureidoglycolate content upon allantoate feeding. A, Reverse transcription-PCR of soybean RNA extracted from leaves of independent plants that were either mock inoculated (mock) or inoculated with DNA coding for wild-type *Bean pod mottle virus* (BPMV; control) or with DNA coding for three different BPMV-uah viral RNAs. Leaves from two to three independent plants were analyzed in each case. Two different primer pairs were used for the detection of *UAH* transcript (Supplemental Table S1). B, *UAH* protein amounts in pools of the biological replicates shown in A analyzed by western blot with *UAH*-specific antiserum. C, Ureidoglycolate content before and 8 h after feeding of 10 mM racemic allantoate via the petiole. Values shown are means of two (mock) or three (other samples) biological replicates. Error bars are sd. FW, Fresh weight.

Subcellular Location of Soybean and Arabidopsis UAH

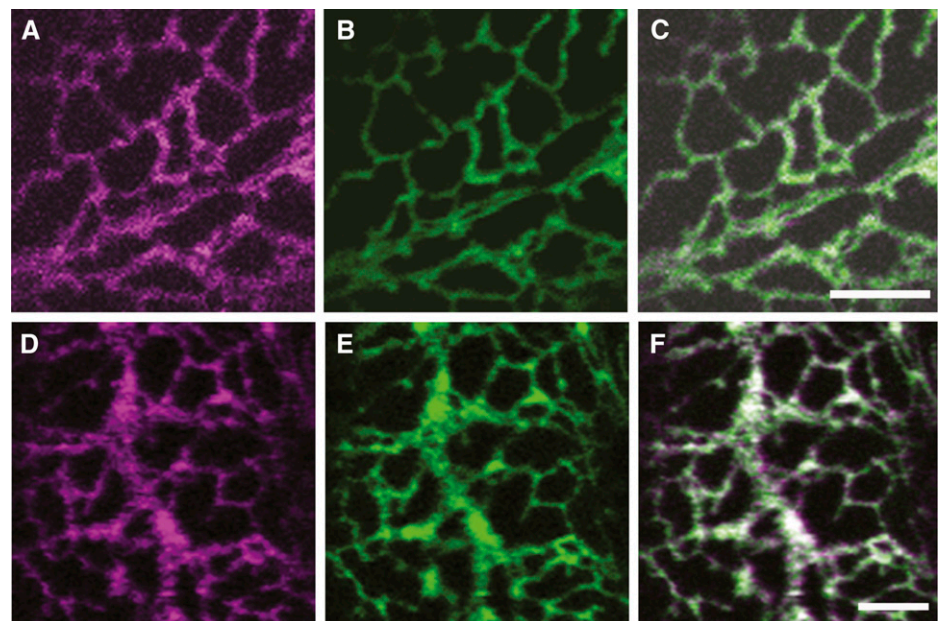
ALN and AAH of Arabidopsis and soybean as well as UGlyAH of Arabidopsis were previously shown to reside in the ER (Werner et al., 2008; Serventi et al., 2010). It is likely that the ureidoglycolate-degrading enzyme also resides in the ER to avoid the transport of the unstable ureidoglycolate. UAH from Arabidopsis and soybean fulfill this requirement (Fig. 7), in agreement with a role of UAH in ureidoglycolate catabolism *in vivo*. UAH generally locates to the ER but is very occasionally also found in the Golgi and the peroxisomes (Supplemental Fig. S12), as observed previously for ALN and AAH as well (Werner et al., 2008).

DISCUSSION

It has been known for decades that some plants utilize the purine-derived ureides allantoin and allantoate as nitrogen transport compounds (Bollard, 1957; Reinbothe and Mothes, 1962; Thomas and Schrader, 1981). In certain legumes, like soybean and common bean, these ureides are synthesized from fixed nitrogen in the nodules and exported to the shoot (Matsumoto et al., 1977a; Schubert, 1986). Under nonfixing conditions, significantly less ureides are found in the xylem (McClure and Israel, 1979; do Amarante et al., 2006). During germination, ureides possibly serve to export nitrogen from the cotyledons to the shoot axis (Quiles et al., 2009; Duran and Todd, 2012), and during senescence, they remobilize nitrogen from the vegetative tissue to the seeds (Thomas et al., 1980; Aveline et al., 1995; Díaz-Leal et al., 2012). When ureides are utilized as transport compounds, they must be taken up and hydrolyzed in the target tissue to gain access to the nitrogen. A complete pathway for ureide degradation in Arabidopsis, including the genetic

identification and biochemical characterization of all enzymes involved, has been suggested recently (Werner et al., 2010). However, evidence demonstrating that UGlyAH and UAH are part of ureide catabolism *in vivo* was still lacking, and the matter remained controversial. Here, we demonstrate that UAH is required for ureidoglycolate hydrolysis in Arabidopsis and that AAH and UAH are needed in soybean. The involvement of UAH implies an *in vivo* role for UGlyAH, because this enzyme is necessary to connect the AAH and UAH reactions (Fig. 3; Werner et al., 2010). The subcellular location of UGlyAH in the ER (Serventi et al., 2010; I.A. Sparkes and C.-P. Witte, unpublished data) is consistent with its role in ureide degradation, because the unstable substrate of this enzyme, *S*-ureidoglycine, is generated by AAH in the same organelle (Werner et al., 2008). A further line of evidence is the tight genetic linkage between *AAH* and *UGlyAH* genes in several bacterial genomes, implying a functional relationship between these two enzymes. This argument cannot be extended to UAH, as it is currently uncertain if UAH orthologs exist in bacteria (Werner et al., 2010). The amidohydrolase pathway of ureide degradation is universally present in plants, because genes for orthologous enzymes are found in all plant genomes sequenced to date. For one monocotyledonous species (rice), it was demonstrated here that such orthologs are functional. Also, some algae like *C. reinhardtii* possess the genes for this pathway, whereas others, such as *Ostreococcus lucimarinus*, lack them. The capability to remobilize nitrogen from purine nucleobases may not be strictly required in unicellular organisms, which do not need to shift nutrients from source to sink tissues. In these organisms, the pathway may serve to use external purines as nitrogen source.

Figure 7. Subcellular localization of AtUAH and GmUAH in tobacco leaf epidermal cells. AtUAH-YFP (A and C; magenta) and GmUAH-YFP (D and F; magenta) were transiently coexpressed in tobacco leaf epidermal cells with an ER marker, GFP-HDEL (B, C, E, and F; green). Merged images (C and F) indicate that UAHs from Arabidopsis and soybean locate to the ER. Bars = 5 μ m.



Evidence for a possible adaptation of certain ureide catabolic isoenzymes to the particular ureide metabolism of soybean was not found in this study. The genome of common bean only codes for single copies of *AAH*, *UGlyAH*, and *UAH*, arguing against a requirement for multiple gene copies of these genes in ureide-exporting legumes. However, there are two *ALN* genes in the genome of common bean, *PvALN1* and *PvALN2*. *PvALN2* is most similar to *ALN3* and *ALN4* from soybean, and as with these, its transcript is almost exclusively present in the nodules (Díaz-Leal et al., 2012). Interestingly, the transcript of *PvALN2* contains one out-of-frame and two in-frame AUG codons upstream of the predicted start codon in the 5' leader sequence (according to data from Phytozome V8 [www.phytozome.net]), indicating that, like the soybean orthologs, it may not be efficiently translated. To decide finally on the function of these nodule-specific *ALNs* of ureide-exporting legumes, evidence from studies with mutants will be required. Such evidence was needed, for example, to demonstrate that one of the two copies of urease accessory protein F (*UreF*) of soybean was sufficient for almost all in vivo activity, although both *UreF* genes of this plant are equally transcribed and both proteins are functional (Polacco et al., 2011). Mutations in 5' leader sequences resulting in inefficient translation may be especially selected after gene or (partial) genome duplications, as had occurred in soybean (Kim et al., 2009). Such mutations lower the protein dose without producing aberrant proteins, while transcriptional patterns, which are more complex to change, can be maintained.

Surprisingly, neither the source of nitrogen nor the concentration of ureides had a marked impact on the transcript or the protein abundance of the investigated ureide-degrading enzymes in soybean. The relative independence of ureide-degrading activities and transcript amounts for *ALN* and *AAH* from environmental conditions, in particular the status of nitrogen fixation, had been noted earlier (Charlson et al., 2009; Alamillo et al., 2010; Díaz-Leal et al., 2012). *ALN* activity was independent of tissue ureide influx and ureide content, while *AAH* activity was only about 50% lower in soybean plants not relying on fixed nitrogen (Winkler et al., 1988; Rice et al., 1990). In contrast, Duran and Todd (2012) reported that *ALN* transcripts as well as activity were increased in several tissues of soybean relying on nitrogen fixation compared with nonfixing controls. However, it remains an open question how ureide catabolism is regulated to coordinate carbon and nitrogen metabolism in soybean plants depending on nitrogen fixation. One possible option is a translational or posttranslational regulation of *AAH* serving as a pacemaker for ureide degradation. It appears plausible that regulation acts on *AAH* (and not *ALN*, *UGlyAH*, or *UAH*) because (1) most ureide nitrogen is exported as allantoate and not allantoin from the nodules and (2) allantoate is a stable compound whereas allantoate degradation products rapidly decay, leading to the release of ammonia. An alternative option is that allantoin and allantoate are stored isolated from their site of degradation,

while the store may be connected to a regulated transport mechanism that delivers ureides to the catabolic enzymes on demand (Winkler et al., 1988). These interesting questions of regulation and coordination of nitrogen and carbon metabolism will be the subject of future studies.

MATERIALS AND METHODS

Arabidopsis Mutants and Complementation Lines

The following *Arabidopsis thaliana* variants were used: *aln* mutant, SAIL 810E12 (Werner et al., 2008), *aah* mutant, SALK 112631 (Todd and Polacco, 2006; Werner et al., 2008), *uah* mutant, SALK 024998, and *ure* mutant, SALK 038002 (Witte et al., 2005); *aah ure* and *uah ure* double mutants obtained by crossing the respective single mutants; complementation lines with homozygous transgene insertions: *aln* mutant complemented with 35S-*AtALN-HAS*trep (Werner et al., 2008), *aln* mutant complemented with 35S-*AtAAH-HAS*trep (Werner et al., 2008), and *uah* mutant complemented with 35S-*AtUAH-HAS*trep; and complementation lines with segregating transgene insertions: *aah* mutant with 35S-*GmAAH2-HAS*trep and *uah* mutant with 35S-*GmUAH-HAS*trep (Supplemental Methods S1).

Phenotype and Metabolite Analyses of Arabidopsis Lines

Plants were grown on 0.8% (w/v) agar plates containing one-half-strength Murashige and Skoog nutrients (Murashige and Skoog modified basal salt mixture without nitrogen, phosphorus, and potassium from PhytoTechnology Laboratories), 1.25 mM K_2HPO_4 , 10 mM allantoin, and 0.05% (w/v) MES (pH 5.7) in a growth chamber (KBW 5.1; Binder) at 22°C in the light (14 h) and 19°C in the dark (10 h). After 6 weeks of growth, photographs were taken and 4 × 10 seedlings were harvested, lyophilized, and the dry weight determined.

For the metabolite analysis, the plants were grown on soil (Jiffy-7; Jiffy Products International) in a growth chamber set to 60% humidity (AR-36L3; Percival Scientific) at 22°C in the light (14 h) and 19°C in the dark using only half of the lamps. For lines with segregating transgenes (see above), only plants expressing the transgene were used for analysis (tested by western blot). After 4 weeks, the rosettes from five plants per line (150 mg per rosette) were frozen in liquid nitrogen. For the extraction of the metabolites, 750 μ L of Na_2HPO_4 - KH_2PO_4 buffer (20 mM, pH 7.0) was added, and the material was ground using a rotating pestle. After centrifugation for 15 min (20,000g, 4°C), 700 μ L of supernatant was diluted 1:2 in the phosphate buffer. Twenty microliters was used for the detection of allantoin, allantoate, ureidoglycolate, and glyoxylate (Vogels and Van der Drift, 1970). To 400 μ L of supernatant, 40 μ L of URE (type IX from jack bean [*Canavalia ensiformis*; Sigma-Aldrich] at 4 units μ L⁻¹ in 10 mM HEPES, pH 8.0) was added and incubated at 30°C for 30 min to convert urea to ammonia. This URE-treated supernatant (440 μ L) and 400 μ L of untreated supernatant were loaded on cation-exchange columns (Bond Elut SCX HF [50 mg, 1 mL]; Varian) to separate the ammonia from the extracts. The ammonia was eluted from the columns using 400 μ L of KCl (4 M), and 100 μ L of these fractions was used for the quantification of ammonia and ammonia + urea as described by Witte et al. (2002).

Protein Expression, Extraction, Purification, and Detection

Strep-tagged proteins were transiently expressed in *Nicotiana benthamiana* and affinity purified as described previously (Werner et al., 2008). Yellow fluorescent protein (YFP)-tagged proteins were expressed in tobacco (*Nicotiana tabacum*) together with marker proteins and analyzed by confocal microscopy as described by Werner et al. (2008). Protein extraction from frozen soybean (*Glycine max*) tissues (10 mg) was performed using the extraction conditions described by Werner et al. (2008). Eight micrograms of protein was loaded per lane on SDS gels. SDS gel electrophoresis, Coomassie blue staining, silver staining, and western-blot analyses were performed according to Witte et al. (2004). StrepTactin alkaline phosphatase conjugate (IBA) was diluted 1:4,000 for the detection of StrepII-tagged proteins. Native soybean proteins were detected using rabbit serum containing polyclonal antibodies raised against GmALN1, AtAAH, GmUGlyAH1, and AtUAH. The antisera were commercially produced (Biogenes) using the corresponding C-terminally His-tagged

proteins expressed in *Escherichia coli* purified with metal affinity chromatography under denaturing conditions.

Enzymatic Activities

The activity measurement of the soybean enzymes (Fig. 3) was performed as described by Werner et al. (2010). For determination of the kinetic constants, the activities of all enzymes were measured at 30°C within 3 min in triplicate. For the ALNs, 5 μ L of freshly purified enzymes was incubated with 15 μ L of racemic allantoin at concentrations of 2.5, 5, 10, 20, 40, and 80 mM. The reactions were stopped by adding 60 μ L of water and 20 μ L of HCl (0.15 M) on ice, and the production of allantoin was determined according to Vogels and Van der Drift (1970). For the AAHs, the assay procedure described by Werner et al. (2008), with allantoin concentrations of 37.5, 75, 150, 300, 600, and 1,200 μ M, was used to determine ammonia directly in the 200- μ L reaction mixtures. For the UAHs, racemic ureidoglycolate at 75, 150, 300, 600, 1,200, and 2,400 μ M was used as substrate, and the production of glyoxylate was quantified directly in 100- μ L reaction mixtures after the addition of 20 μ L of EDTA (100 mM) to stop the enzymatic reactions (Vogels and Van der Drift, 1970). For activity measurements of soybean UGlyAH see Supplemental Methods S1.

Soybean Growth Conditions

Soybean (cv Williams 82) seeds were germinated in a wet perlite:vermiculite mixture (1:1, v/v) for 5 to 7 d. For experiments where nitrogen-fixing plants were compared with plants growing without nitrogen fixation, plantlets were transferred to pots containing the same mixture and fertilized with nutrient solutions prepared according to Todd and Polacco (2004). Plants for silencing experiments were grown on fertilized soil. All plants grew with a photoperiod of 16 h of light (Osram Lumilux 865 lamps; 26°C) and 8 h of dark (20°C) at 80% humidity in a growth chamber (KBWF E5.2; Binder). For nitrogen-fixing plants, *Bradyrhizobium japonicum* 110spc4 (Regensburger and Hennecke, 1983) was added after germination.

Reverse Transcription-PCR Analyses

Total RNA from several soybean tissues was extracted employing the TRIzol reagent (Biolone). Typically, 1 μ g of total RNA was reverse transcribed using the *Moloney murine leukemia virus* enzyme (Promega). PCR was performed using *Taq* DNA polymerase (New England Biolabs) with the gene-specific primers listed in Supplemental Table S1. The transcript from the *CYP2* housekeeping gene (Glyma12g02790) served as control.

RNA Ligase-Mediated-RACE PCR

The FirstChoice RLM-RACE Kit (Ambion, Invitrogen) was used according to the manufacturer's instructions to clone the 5' end of soybean *ALN3* and *ALN4* transcripts. Total RNA either from the apical shoot tip or nodule was used as a starting material. Gene-specific primers used in outer and inner PCR amplifications are listed in Supplemental Table S1. Amplified products were cloned into pJet1.2 (Fermentas), and several independent clones were sequenced.

Ureide Analysis from Soybean Tissues

Leaf material (10 mg, 7-mm disc) was harvested, frozen in liquid nitrogen, and ground in a mill (MM400; Retsch) for 2 min at 30 s⁻¹ using ceramic beads. The metabolites were extracted with 100 μ L of Na₂HPO₄-KH₂PO₄ buffer (20 mM, pH 7.0) containing 5 mM EDTA, and debris was removed by centrifugation (1 min, 16,000g). Because the soybean extracts interfered with those reactions requiring NaOH in the differential glyoxylate assay for ureide quantification (Vogels and Van der Drift, 1970), a modified protocol was used. For the measurement of allantoin and allantoate, extracts were diluted 1:10 in the phosphate buffer, diluting out the interference. Ureidoglycolate was converted enzymatically to glyoxylate and urea using a ureidoglycolate urea hydrolase from *E. coli* prepared as described by Werner et al. (2010) but frozen directly in desalting buffer (100 mM HEPES, pH 8.0, 100 mM NaCl, 0.5 mM EDTA, and 0.005% [v/v] Triton X-100). Samples of 20 μ L were processed for each metabolite according to the detailed pipetting scheme in Supplemental Table S2.

After conversion of the ureides, 20 μ L of phenylhydrazine (6.6 mg in 2 mL of water) was added, incubated for 5 min at room temperature and 5 min on

ice, followed by the addition of 100 μ L of HCl (37%) and 20 μ L of potassium ferricyanide (III) (33.3 mg in 2 mL of water). The absorbance was measured at 537 nm (Vogels and Van der Drift, 1970).

VIGS in Soybean

To silence the soybean genes, the bean pod mottle virus vectors pBPMV-IA-R1M (RNA 1) and pBPMV-IA-V1 (RNA 2; Zhang et al., 2010) were used. For silencing of the two *GmAAH* genes, an *AAH* fragment was amplified by PCR (for primers, see Supplemental Table S1) and cloned into the *Bam*HI site of pBPMV-IA-V1. For *GmUAH* silencing, three different *GmUAH1* fragments were amplified and cloned via *Bam*HI into pBPMV-IA-V1. In all cases, constructs with antisense orientation of *UAH* or *AAH* were selected. DNA rubbing onto primary leaves of soybean seedlings was performed according to Zhang et al. (2010), and typically, 1 μ g of DNA was used as leaf inoculum. Three to 4 weeks after inoculation, systemic leaves showing symptoms were collected and stored at -80°C for further analysis.

Feeding of Soybean Leaves

Petioles of selected leaves were cut under water in the morning and then transferred to 2-mL tubes filled with a solution containing 10 mM racemic allantoin, 10 mM HEPES (pH 8.0), and 5 μ M MnCl₂. Leaves were incubated at 26°C in a growth chamber (KBW 3.1; Binder) under continuous light during the 8-h feeding period. At the indicated time points, leaf disc samples were taken, immediately frozen, and stored at -80°C.

For the locus numbers of the ureide catabolic genes discussed, see Supplemental Figure S1. The locus number for *URE* is At1g67550.

Supplemental Data

The following materials are available in the online version of this article.

Supplemental Figure S1. Scheme of ureide generation and catabolism in soybean.

Supplemental Figure S2. Assessment of *UAH* transcript amounts in the *uah* T-DNA mutant.

Supplemental Figure S3. Multiple alignment of ALNs from plants, algae, *Saccharomyces cerevisiae*, *E. coli*, and *Bacillus subtilis*.

Supplemental Figure S4. Multiple alignment of AAHs from higher plants, the moss *P. patens*, and the alga *C. reinhardtii*.

Supplemental Figure S5. Multiple alignment of UGlyAHs from higher plants, the moss *P. patens*, and the alga *C. reinhardtii*.

Supplemental Figure S6. Multiple alignment of UAHs from higher plants, the moss *P. patens*, and the alga *C. reinhardtii*.

Supplemental Figure S7. Proteins with C-terminal Strep-tag affinity purified after transient expression in *N. benthamiana*.

Supplemental Figure S8. AAH, UGlyAH, and UAH from rice: affinity-purified proteins and enzymatic activity.

Supplemental Figure S9. Acceleration of ammonia release from allantoin in the *GmAAH* reaction by *GmUGlyAH1* or *GmUGlyAH2*.

Supplemental Figure S10. Expression profiles of the ureide catabolic genes of soybean extracted from publicly available data (RNAseq).

Supplemental Figure S11. Expression of ureide catabolic genes/proteins as well as ureide content in older (second) and younger (third) leaves of soybean plants in the early V3 stage under different nitrogen regimes.

Supplemental Figure S12. Alternative subcellular locations of AtUAH-YFP in tobacco leaf epidermal cells.

Supplemental Table S1. List of primers used in this work.

Supplemental Table S2. Pipetting and incubation scheme for ureide conversion to glyoxylate in a differential glyoxylate analysis adapted for soybean metabolite extracts.

Supplemental Methods S1. Cloning details, *uah1* mutant analysis and complementation, assessment of soybean UGlyAH activity.

ACKNOWLEDGMENTS

We thank Renate Grübner, Ruth Lintermann, Karla Dünnbier, und Silke Schilling for technical and logistical support.

Received July 1, 2013; accepted August 11, 2013; published August 12, 2013.

LITERATURE CITED

- Alamillo JM, Díaz-Leal JL, Sánchez-Moran MV, Pineda M (2010) Molecular analysis of ureide accumulation under drought stress in *Phaseolus vulgaris* L. *Plant Cell Environ* **33**: 1828–1837
- Aveline A, Crozat Y, Pinochet X, Domenach AM, Cleyetmarel JC (1995) Early remobilization: a possible source of error in the ureide assay-method for N-2 fixation measurement by early-maturing soybean. *Soil Sci Plant Nutr* **41**: 737–751
- Bollard EG (1957) Translocation of organic nitrogen in the xylem. *Aust J Biol Sci* **10**: 292–301
- Charlson DV, Korth KL, Purcell LC (2009) Allantoate amidohydrolase transcript expression is independent of drought tolerance in soybean. *J Exp Bot* **60**: 847–851
- Collier R, Tegeder M (2012) Soybean ureide transporters play a critical role in nodule development, function and nitrogen export. *Plant J* **72**: 355–367
- Desimone M, Catoni E, Ludewig U, Hilpert M, Schneider A, Kunze R, Tegeder M, Frommer WB, Schumacher K (2002) A novel superfamily of transporters for allantoin and other oxo derivatives of nitrogen heterocyclic compounds in *Arabidopsis*. *Plant Cell* **14**: 847–856
- Díaz-Leal JL, Gálvez-Valdivieso G, Fernández J, Pineda M, Alamillo JM (2012) Developmental effects on ureide levels are mediated by tissue-specific regulation of allantoinase in *Phaseolus vulgaris* L. *J Exp Bot* **63**: 4095–4106
- do Amarante L, Lima JD, Sodek L (2006) Growth and stress conditions cause similar changes in xylem amino acids for different legume species. *Environ Exp Bot* **58**: 123–129
- Duran VA, Todd CD (2012) Four allantoinase genes are expressed in nitrogen-fixing soybean. *Plant Physiol Biochem* **54**: 149–155
- Gravenmade EJ, Vogels GD, Van der Drift C (1970) Hydrolysis, racemization and absolute configuration of ureidoglycolate, a substrate of allantoinase. *Biochim Biophys Acta* **198**: 569–582
- Hesberg C, Hänsch R, Mendel RR, Bittner F (2004) Tandem orientation of duplicated xanthine dehydrogenase genes from *Arabidopsis thaliana*: differential gene expression and enzyme activities. *J Biol Chem* **279**: 13547–13554
- Hinnebusch AG (2011) Molecular mechanism of scanning and start codon selection in eukaryotes. *Microbiol Mol Biol Rev* **75**: 434–467
- Juvalle PS, Hewezi T, Zhang CQ, Kandath PK, Mitchum MG, Hill JH, Whitham SA, Baum TJ (2012) Temporal and spatial bean pod mottle virus-induced gene silencing in soybean. *Mol Plant Pathol* **13**: 1140–1148
- Kim KD, Shin JH, Van K, Kim DH, Lee SH (2009) Dynamic rearrangements determine genome organization and useful traits in soybean. *Plant Physiol* **151**: 1066–1076
- Kozak M (1991) A short leader sequence impairs the fidelity of initiation by eukaryotic ribosomes. *Gene Expr* **1**: 111–115
- Lamberto I, Percudani R, Gatti R, Foli C, Petrucco S (2010) Conserved alternative splicing of *Arabidopsis* transthyretin-like determines protein localization and S-allantoin synthesis in peroxisomes. *Plant Cell* **22**: 1564–1574
- Masclaux C, Valadier MH, Brugière N, Morot-Gaudry JF, Hirel B (2000) Characterization of the sink/source transition in tobacco (*Nicotiana tabacum* L.) shoots in relation to nitrogen management and leaf senescence. *Planta* **211**: 510–518
- Masclaux-Daubresse C, Daniel-Vedele F, Dechorgnat J, Chardon F, Gauffichon L, Suzuki A (2010) Nitrogen uptake, assimilation and remobilization in plants: challenges for sustainable and productive agriculture. *Ann Bot (Lond)* **105**: 1141–1157
- Matsumoto T, Yatazawa M, Yamamoto Y (1977a) Incorporation of N-15 into allantoin in nodulated soybean plants supplied with N-15(2). *Plant Cell Physiol* **18**: 459–462
- Matsumoto T, Yatazawa M, Yamamoto Y (1977b) Distribution and change in contents of allantoin and allantoic acid in developing nodulating and non-nodulating soybean plants. *Plant Cell Physiol* **18**: 353–359
- McClure PR, Israel DW (1979) Transport of nitrogen in the xylem of soybean plants. *Plant Physiol* **64**: 411–416
- Muñoz A, Piedras P, Aguilar M, Pineda M (2001) Urea is a product of ureidoglycolate degradation in chickpea: purification and characterization of the ureidoglycolate urea-lyase. *Plant Physiol* **125**: 828–834
- Muñoz A, Raso MJ, Pineda M, Piedras P (2006) Degradation of ureidoglycolate in French bean (*Phaseolus vulgaris*) is catalysed by a ubiquitous ureidoglycolate urea-lyase. *Planta* **224**: 175–184
- Polacco JC, Hyten DL, Medeiros-Silva M, Slepser DA, Bilyeu KD (2011) Mutational analysis of the major soybean UreF paralogue involved in urease activation. *J Exp Bot* **62**: 3599–3608
- Quiles FA, Raso MJ, Pineda M, Piedras P (2009) Ureide metabolism during seedling development in French bean (*Phaseolus vulgaris*). *Physiol Plant* **135**: 19–28
- Regensburger B, Hennecke H (1983) RNA polymerase from *Rhizobium japonicum*. *Arch Microbiol* **135**: 103–109
- Reinbothe H, Mothes K (1962) Urea, ureides, and guanidines in plants. *Annu Rev Plant Physiol Plant Mol Biol* **13**: 129–150
- Rice CF, Lukaszewski KM, Walker S, Blevins DG, Winkler RG, Randall DD (1990) Changes in ureide synthesis, transport and assimilation following ammonium-nitrate fertilization of nodulated soybeans. *J Plant Nutr* **13**: 1539–1553
- Schubert KR (1981) Enzymes of purine biosynthesis and catabolism in *Glycine max*. 1. Comparison of activities with N-2 fixation and composition of xylem exudate during nodule development. *Plant Physiol* **68**: 1115–1122
- Schubert KR (1986) Products of biological nitrogen-fixation in higher-plants: synthesis, transport, and metabolism. *Annu Rev Plant Physiol Plant Mol Biol* **37**: 539–574
- Serventi F, Ramazzina I, Lamberto I, Puggioni V, Gatti R, Percudani R (2010) Chemical basis of nitrogen recovery through the ureide pathway: formation and hydrolysis of S-ureidoglycine in plants and bacteria. *ACS Chem Biol* **5**: 203–214
- Severin AJ, Woody JL, Bolon YT, Joseph B, Diers BW, Farmer AD, Muehlbauer GJ, Nelson RT, Grant D, Specht JE, et al (2010) RNA-Seq atlas of *Glycine max*: a guide to the soybean transcriptome. *BMC Plant Biol* **10**: 160
- Stebbins NE, Polacco JC (1995) Urease is not essential for ureide degradation in soybean. *Plant Physiol* **109**: 169–175
- Thomas RJ, Feller U, Erismann KH (1980) Ureide metabolism in non-nodulated *Phaseolus vulgaris* L. *J Exp Bot* **31**: 409–417
- Thomas RJ, Schrader LE (1981) Ureide metabolism in higher plants. *Phytochemistry* **20**: 361–371
- Todd CD, Polacco JC (2004) Soybean cultivars ‘Williams 82’ and ‘Maple Arrow’ produce both urea and ammonia during ureide degradation. *J Exp Bot* **55**: 867–877
- Todd CD, Polacco JC (2006) AtAAH encodes a protein with allantoinase amidohydrolase activity from *Arabidopsis thaliana*. *Planta* **223**: 1108–1113
- Vogels GD, Van der Drift C (1970) Differential analyses of glyoxylate derivatives. *Anal Biochem* **33**: 143–157
- Werner AK, Romeis T, Witte CP (2010) Ureide catabolism in *Arabidopsis thaliana* and *Escherichia coli*. *Nat Chem Biol* **6**: 19–21
- Werner AK, Sparkes IA, Romeis T, Witte CP (2008) Identification, biochemical characterization, and subcellular localization of allantoinase amidohydrolases from *Arabidopsis* and soybean. *Plant Physiol* **146**: 418–430
- Werner AK, Witte CP (2011) The biochemistry of nitrogen mobilization: purine ring catabolism. *Trends Plant Sci* **16**: 381–387
- Winkler RG, Blevins DG, Polacco JC, Randall DD (1987) Ureide catabolism of soybeans. II. Pathway of catabolism in intact leaf tissue. *Plant Physiol* **83**: 585–591
- Winkler RG, Blevins DG, Polacco JC, Randall DD (1988) Ureide catabolism in nitrogen-fixing legumes. *Trends Biochem Sci* **13**: 97–100
- Winkler RG, Polacco JC, Blevins DG, Randall DD (1985) Enzymic degradation of allantoin in developing soybeans. *Plant Physiol* **79**: 787–793
- Witte CP, Noël LD, Gielbert J, Parker JE, Romeis T (2004) Rapid one-step protein purification from plant material using the eight-amino acid StrepII epitope. *Plant Mol Biol* **55**: 135–147
- Witte CP, Rosso MG, Romeis T (2005) Identification of three urease accessory proteins that are required for urease activation in *Arabidopsis*. *Plant Physiol* **139**: 1155–1162
- Witte CP, Tiller SA, Taylor MA, Davies HV (2002) Leaf urea metabolism in potato: urease activity profile and patterns of recovery and distribution of ¹⁵N after foliar urea application in wild-type and urease-antisense transgenics. *Plant Physiol* **128**: 1129–1136
- Yang J, Han KH (2004) Functional characterization of allantoinase genes from *Arabidopsis* and a nonureide-type legume black locust. *Plant Physiol* **134**: 1039–1049
- Zhang C, Bradshaw JD, Whitham SA, Hill JH (2010) The development of an efficient multipurpose bean pod mottle virus viral vector set for foreign gene expression and RNA silencing. *Plant Physiol* **153**: 52–65
- Zrenner R, Riegler H, Marquard CR, Lange PR, Geserick C, Bartosz CE, Chen CT, Slocum RD (2009) A functional analysis of the pyrimidine catabolic pathway in *Arabidopsis*. *New Phytol* **183**: 117–132